Water Research X 7 (2020) 100049

Contents lists available at ScienceDirect

Water Research X

journal homepage: https://www.journals.elsevier.com/water-research-x

Quantifying clogging patterns of infiltration systems to improve urban stormwater pollution reduction estimates

Gary Conley [a, *], Nicole Beck [a], Catherine A. Riihimaki [b], Michelle Tanner [a]

[a] 2NDNATURE, 500 Seabright Avenue, Santa Cruz, CA, 95062, USA
[b] Princeton University, Council on Science and Technology, 234 Lewis Library, Princeton, NJ, 08544, USA

ARTICLE INFO

Article history:
Received 23 December 2019
Received in revised form
7 March 2020
Accepted 7 March 2020
Available online 9 March 2020

Keywords:
Stormwater
BMP
Modeling
Infiltration
Clogging

ABSTRACT

Infiltration systems are among the most commonly implemented practices to control urban stormwater and to attenuate pollutant delivery to receiving waters, because they are relatively cheap to build and amenable to space constraints in urbanized areas. However, infiltration systems tend to clog with sediments, which can rapidly reduce their performance. While clogging has been consistently identified as a significant determinant on infiltration BMP (best management practice) performance and lifespan, there have been few methods reported to predict rates of clogging or incorporate insights to urban catchment water quality modeling. We ran a series of laboratory and field experiments to identify clogging mechanisms and quantify infiltration performance declines as a function of sediment loading. The results show rapid initial declines of infiltration rate, primarily due to accumulation of material at the bottom of the infiltration BMP. The performance decline trajectories were sensitive to BMP geometry, with BMPs that had greater lateral infiltration surface area declining less quickly. We integrated these experimental results to a spatially distributed stormwater model to illustrate how they can be used to predict BMP performance declines over time and assess cost trade-offs. Results will be used to adapt algorithms in a cloud-based stormwater management platform to better inform maintenance needs for cities and improve the accuracy of urban stormwater pollutant load reduction estimates that support regulatory compliance tracking.

1. Introduction

Stormwater runoff from cities causes declines in water quality downstream (Arnold and Gibbons, 1996; Holman-Dodds et al., 2003; US EPA, 2013) from the expansion of impervious cover (Booth and Jackson, 1997), which disrupts the natural hydrologic cycle and enhances the entrainment and transport of sediment, nutrients, bacteria, metals, pesticides, and other chemicals derived from urban land uses (Grove et al., 2001; Tang et al., 2005; US EPA, 2013). As part of their compliance with non-point source pollutant discharge (NPDES) requirements, municipalities implement structural controls, known as best management practices (BMPs), to reduce runoff and urban pollutant loading to receiving waters. A wide range of structural BMPs, such as infiltration trenches, infiltration basins, dry wells, or bioretention systems, rely on filtration of stormwater through media and underlying soil to reduce pollution impacts (Brander et al., 2004; Bedan and Clausen, 2009; Gilroy and McCuen, 2009; Ahiablame et al., 2012).

Infiltration trenches are practical structural solutions in urban areas for their ability to fit in available spaces, particularly if runoff can be delivered by underground pipe (Burton and Pitt, 2002). A disadvantage of infiltration structures is that they tend to clog up with sediments, which fill pore spaces, dramatically reducing their infiltration performance (Freni et al., 2010; Furumai et al., 2005; Lindsey et al., 1992; Hatt et al., 2007), often within a short period of time (Ellis, 2000). While infiltration BMPs observed in the field may show substantial performance degradation due to accumulation of material (Le Coustumer and Barraud, 2006), in practice, they are rarely monitored after installation (National Research Council, 2008). Field studies have shown wide variation of clogging rates (Toran and Jedrzejczyk, 2017), in part due to variations in poorly constrained local conditions (Potter, 2006). As city populations swell and the urbanized landscape expands, the number of structural BMPs needed to mitigate stormwater runoff impacts on local receiving waters will grow. The accurate identification of structural BMP maintenance needs is critical for cities to prioritize how they

* Corresponding author.
E-mail address: gary@2ndnaturewater.com (G. Conley).

https://doi.org/10.1016/j.wroa.2020.100049

spend limited resources to ensure that the water quality benefits from structural BMPs continue after installation (e.g. Nozi et al., 1999). BMPs require maintenance at varying frequencies that depend on BMP type and runoff characteristics, such as sediment concentration and total cumulative loading (Mercado et al., 2015). However, there are no generally accepted methods to predict clogging despite consistent acknowledgment of its importance in both laboratory experiments (Le Coustumer and Barraud, 2006; Pokrajac and Deletic, 2002) and modeling studies (Freni et al., 2010; Browne et al., 2007).

Stormwater managers are increasingly being required to demonstrate pollutant load reduction effectiveness of their programs as part of their NPDES reporting requirements (e.g. US EPA, 2018). Cities typically rely on modeling or estimation methods to gauge effectiveness (US EPA, 2017). Although a comparative study from Furumai et al. (2005) concluded that the clogging phenomenon must be included for a correct simulation of infiltration BMPs, there remain very few modeling methods that account for clogging of infiltration systems. Examples of methods that do include clogging are provided by Dechesne et al. (2005) and Siriwardene (2007b, 2007c). Commonly used catchment modeling platforms in the United States such as SWMM (Rossman et al., 2015), SUSTAIN (Shoemaker et al., 2009), and BASINS (US EPA, 2019) typically rely on the assumption that BMPs continue to function in perpetuity at their optimal performance level. As a result, most catchment-based stormwater modeling does not account for the degradation of structural BMP performance over time due to clogging (Freni et al., 2010). The implication of such assumptions results is unrealistic expectations of long-term water quality benefits and de-emphasizes the critical role structural BMP maintenance plays in sustaining delivery of the urban water quality improvements.

Few studies are available that quantify the impacts of clogging on BMP performance (e.g. Tu and Traver, 2018; Siriwardene et al., 2007a; Kandra et al., 2014) or dependence of clogging on BMP design parameters (e.g. Le Coustumer et al., 2007). Most methods available are not amendable to incorporation to catchment modeling approaches that include many BMPs with unique settings and designs (Freni et al., 2010). Even recent data synthesis efforts to quantify BMP performance that are explicitly targeted toward stormwater practitioners have not proved useful for predicting infiltration performance declines, since they do not consider infiltration system age, geometry, or loading rates (Clary et al., 2017). Still more vexing is the fact that these efforts cannot identify the primary sources of uncertainty that contribute to BMP performance variance (Afrooz et al., 2019). The current state of knowledge appears little advanced from the findings of Selvakumar et al. (2005), who concluded that structural BMP performance information was difficult to interpret and operationalize due to an array of complex and interrelated parameters along with differences in methods for characterizing effectiveness.

Given that a better understanding of the causes, rates, and magnitude of BMP performance declines over time can improve estimates of pollution reduction progress and allocation of maintenance resources, the objectives of this study are:

1. Identify clogging factors and mechanisms contributing to performance decline of infiltration BMPs
2. Develop a simple method to estimate infiltration BMP performance declines over time that can be integrated into a catchment-scale urban pollutant loading model

To this end, we used outputs from field and laboratory experiments to parameterize small-scale infiltration BMP performance declines for integration to a catchment-based stormwater model.

2. Materials and methods

2.1. Stormwater loading experiments

BMP infiltration rate attenuation in response to stormwater loading was measured via laboratory and field experiments. The laboratory experiments allowed detailed observation of sediment accumulation patterns and clogging mechanisms with sequential stormwater loading, while the field experiments provided infiltration observations in real-world settings, where both the structural heterogeneities and dynamics of the soil wetting front were present. All experiments were run in triplicate to quantify measurement precision for a better basis of comparison.

Loading and infiltration measurement procedures were similar for both the laboratory and field experiments, with differences in the experimental setup (see sections 2.2 and 2.3). Both the laboratory and field experiments used synthetic stormwater created by mixing tap water with material collected from regenerative air street sweeper cartridge filters, which separate out large particles. Sieving of this material indicated that it was all smaller than fine sand (<125 μm) and approximately 50% was smaller than clay-sized particles (<63 μm), and of that fraction, 34% < 32 μm, 27% < 14, and 16% < 8 μm (2NDNATURE and NHC, 2013). This is somewhat finer than the particle sizes used in other studies such as Segismundo et al. (2017), who use material <250 μm. However, fine material has been shown to be a much more influential component than overall sediment mass to explain clogging rates (Siriwardene et al., 2007a), since coarser material tends to settle out before reaching filter media (Kandra et al., 2010). Additionally, for most urban land uses, most of the sedimentary material in urban stormwater may be composed of particles <125 μm, and the majority may be < 63 μm for roads (Selbig, 2015). Synthetic stormwater was poured onto the surface of BMPs, and infiltration rates were measured by noting the height of the water within the BMP at regular time intervals. This was a much simpler procedure compared to previous studies, such as Siriwardene et al. (2007a), who performed a similar experiment for a period of two years and used a continuous tipping gauge at the outflow to measure flow rate.

Trials were conducted to determine reasonable stormwater sediment concentrations and total sediment mass that may be needed to create substantial clogging within a few days of running the experiments. Laboratory experiments used concentrations of 150 mg/L, which is within the range of typical of urban stormwater concentrations (e.g. Fletcher, 2003), while the field experiments, with larger BMPs and more infiltration surface, used concentrations of 2000 mg/L to ensure that there substantial clogging would be observed within the timespan of the experiment. For both experimental setups, prior to taking water level measurements each day, the BMPs were loaded with clean water to saturate the BMP media and surrounding soil/sand. BMPs stormwater loading continued until infiltration rates declined by at least 75% from the initial rate and there was zero or minimal measureable decline in successive measurements.

2.2. Laboratory experimental setup

Three identical enclosures were built from wood and Plexiglass to the specifications shown in Fig. 1 and filled with 2-cm drain rock, which is commonly used as a media for infiltration trenches (Field and Tafuri, 2006). Holes were drilled at the base of the enclosures to allow stormwater to drain into a collection bucket below. Two different BMP geometries were tested in triplicate using these enclosures that we called *Long* and *Mini* (Fig. 1). For each experiment, the drain rock was packed to a

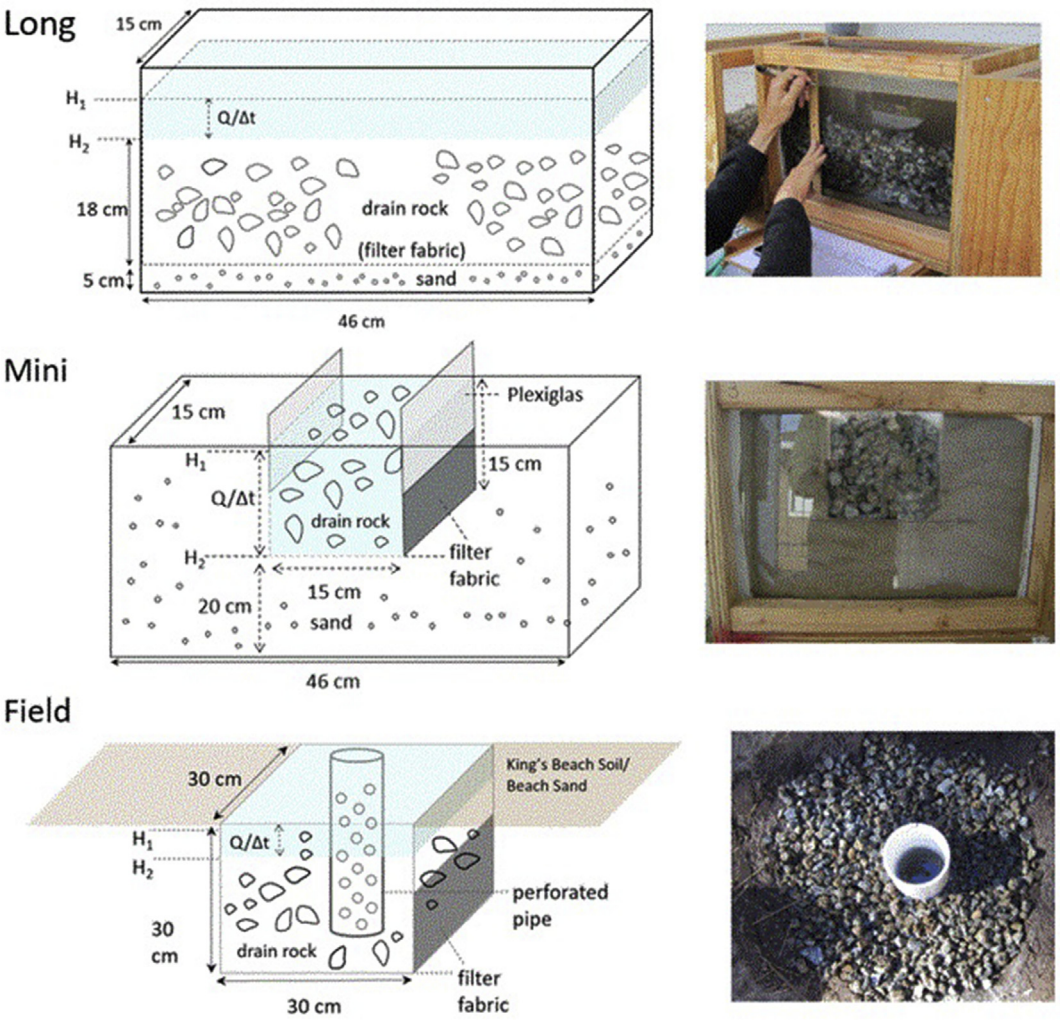

Fig. 1. Laboratory and field experimental BMP setups. Long and Mini laboratory experiments were constructed from wood and Plexiglass with 2 cm drain rock. The Mini experiment had Plexiglass walls sealed in place with removable calking to facilitate stormwater loading. Field experiments at the King's Beach site used a graduated perforated pipe to measure infiltration rates.

consistent density and was surrounded beach sand. Preliminary testing using native soils (Christopher-Gefo series, USDA-NRCS, 2007) did not allow for acceptable precision across the triplicate experiments due to heterogeneity of the soil structure, composition, and differential compaction of the soil samples. These issues were minimized by using beach sand as the surrounding material, rather than soil, which allowed the experiments to isolate the relative differences in infiltration declines between configurations and also allowed stormwater to be loaded into the enclosures more quickly.

The *Long* and *Mini* BMPs were chosen to bracket a range of BMP geometries and to improve understanding of specific elements of BMP clogging. The *Long* configuration (Fig. 1) was designed to isolate the vertical component of infiltration rate decline and to identify differences in infiltration performance decline associated with installation of woven filter fabric at the base of the BMP media (see Fig. 1). Filter fabric is commonly installed in infiltration BMPs to assist with maintenance procedures and is thought to extend the useful lifespan of BMPs. The *Mini* configuration (Fig. 1) was designed to measure the combination of vertical and lateral infiltration rate over time. During each experiment, the location and sediment accumulated within the drain rock and at the infiltration surfaces were recorded and photographed. At the completion of each experiment, the drain rock was carefully extracted from the enclosure to inspect and document the patterns and locations of sediment accumulation.

2.3. Field site experimental setup

The field experiments involved construction of BMPs to estimate infiltration rate declines more comparable to actual BMP field performance, since this setup preserved the influence of surrounding soil structure, compaction variability within the surrounding soil, and development of a more natural wetting front during stormwater loading. Small infiltration BMPs were constructed with square dimensions of 30 cm per side and spaced 2 m apart. For each BMP, approximately 0.027 m^3 of soil was extracted and filled with washed 2-cm drain rock. A 10-cm diameter perforated pipe was installed in the center of each BMP to measure the water draw down rate over time (Fig. 1). Two configurations were tested with three replications each: one with and one without filter fabric placed at the infiltration surface.

The field experiments were conducted during the month of July in the City of Kings Beach, California, USA, and at Seabright Beach in

Santa Cruz, California, USA, to investigate whether degree infiltration decline rates depend upon the initial saturated hydraulic conductivity (K_{sat}) of the surrounding material. The Kings Beach sites are mapped as Kings Beach soil series (USDA-NRCS, 2007) with a measured K_{sat} of approximately 15 cm/h and the Seabright Beach sand, which was intended to represent the upper bound of soil permeability had a measured K_{sat} of approximately 38 cm/h. These experiments included filter fabric, which proved necessary to keep the sand in place so that the holes would not cave in on themselves as drain rock was installed.

2.4. Laboratory sediment loading calculations

For each experiment, we recorded the time required to infiltrate a volume of synthetic stormwater that contained a measured mass of sediment by observing the draw down time of water within the perforated pipe installed in the center of the BMP. Measurements were converted to the BMP's total volumetric discharge rate (Q), which is the product of the BMP length (L_{BMP}) and width (W_{BMP}), the percent void space within the media (V_m) and the change in water depth over time ($\Delta H/t$):

$$Q = (L_{BMP} * W_{BMP} * V_m) * (\Delta H/t) \quad (1)$$

The volumetric discharge (Q) is equivalent to the infiltration rate was expressed as the ratio of the final and initial infiltration rates.

$$Qr = Q_{final}/ Q_{initial} \quad (2)$$

To facilitate comparisons of infiltration rate declines across the different experiments, the cumulative fine sediment loaded to each test BMP was normalized to the infiltration surface area of each BMP.

2.5. Vertical and lateral infiltration components

Experimental results from the laboratory *Long* and *Mini* configurations were used to parse the influence of the BMP geometry on the rate of performance decline. Since the *Long* and *Mini* BMPs were loaded with sediment at the same rate relative to their available infiltration surface, differences in performance at various sediment loading intervals was likely associated with the orientation of the infiltration surfaces. The vertical infiltration component (Qr_v) is equal to that of the *Long* BMP Qr_{long} since there are no lateral infiltration surfaces available in this BMP:

$$Qr_v = Qr_{long} \quad (3)$$

We thus determine the lateral infiltration component (Qr_l) as

$$Qr_l = Qr_{mini} - Qr_{long} \quad (4)$$

where Qr_{mini} is the infiltration rate at a given sediment loading interval of the *Mini* system.

With each of these components discretely defined and plotted as a function of sediment loading per infiltration surface area (g/m^2), we have a way to parameterize infiltration performance decline based on BMP geometry, with separate decline trajectories for vertical and lateral infiltration surfaces as a function of sediment loading. In this way, the net infiltration rate decline of a BMP reflects the proportionality of bottom and side infiltration surfaces.

2.6. Integration of BMP performance declines to a catchment modeling system

We implemented the laboratory results in a set of modeling experiments to illustrate catchment-scale impacts of clogging on distributed BMP runoff reductions and the implications of different BMP geometries. Sediment loading to BMPs was quantified using a modified version of the Stormwater Tool to Estimate Load Reductions (TELR) described in Beck et al. (2017), with two key differences: 1) runoff and sediment generation was spatially distributed at a 30-m grid scale, and 2) we assumed immediate delivery of flows to BMPs, since BMP drainages were small (<0.4 ha) and have high impervious coverage. TELR hydrologic computations use a set of metrics that describe a 30-year rainfall distribution, combined with well-tested algorithms for rainfall-runoff transformation and routing (USDA-SCS, 1986), to generate mean annual runoff estimates for BMP drainages (see Beck et al., 2017). Sediment loading to BMPs was calculated as the product of runoff volumes and constant Total Suspended Solids (TSS) concentrations based on land use. Table 1 lists the runoff concentration values for TSS used in TELR, based on a synthesis of data downloaded from EPA's National Urban Runoff Program database (US EPA, 1983) and the National Stormwater Quality Database (Pitt et al., 2004) and values reported in 23 individual studies (reported in 2NDNATURE, 2017). To account for the proportion of sediment <125 μm (for correspondence with the laboratory experiments), we relied on median values of the data reported by Selbig (2015), and mapping their reported land uses to those used in TELR (Table 1). Particle size distribution estimates from Selbig (2015) show rough correspondence with those from Pitt et al. (2016), who measured 80% of particles in stormwater < 120 μm, and also reports data from US Geologic Survey the show ~85% of particles < 150 μm.

We applied this methodology in the City of Salinas, California, USA, with implementation of 50 infiltration BMPs distributed throughout an urbanized catchment over a period of 10 years. The catchment covered approximately 95 ha and the drainage area captured by all the BMPs accounted for 25% of the total catchment impervious coverage, with and mean impervious coverage for BMP drainages of 57%. Dominant land uses are single family residential, commercial, low, moderate and high traffic roads. We ran 2 scenarios that differed only in the BMP side to bottom area ratios for all BMPs: Shallow (1:1), which is a typical configuration for infiltration BMPs, and Deep (1:4). The relatively simple modeling approach allowed calculation of individual BMP performance decline trajectories and runoff outputs in a manner that reflected both local rates of sediment loading and BMP design. The net relative infiltration rate (Qr_n) of specific BMPs was calculated via the components of vertical and lateral relative infiltration rate (Qr_v and Qr_l, respectively) and the proportion of infiltration area on the bottom and sides of the BMP:

$$Qr_n = (Qr_v * \%Bottom) + (Qr_l * \%Side) \quad (5)$$

Curves were fit to the points resulting from Equation (5) for the BMP geometries at discrete sediment loading intervals and used to predict declines for each BMP included in the simulations. Regardless of geometry, all BMPs were sized such that they captured the runoff generated from the 85th percentile 24-hr rainfall event in Salinas for their drainage area (as estimated by TELR), which is a common design standard to meet low impact development (LID) standards and municipal NPDES permit requirements throughout the United States (US EPA, 2009). Given this volume capture sizing for each BMP, we assumed a constant volume-to-area ratio for both scenarios.

Table 1
Land use TSS characteristic runoff concentrations and sediment fraction <125 μm.

TELR Land use	Reported land use Selbig (2015)	Sediment % <125 μm Selbig (2015)	TELR TSS (<125 μm) concentration (mg/L)
Commercial	Parking lot	90	136
Industrial	Parking lot	90	154
Single family residential	Residential	65	94
Multi-family residential	Residential	65	97
High traffic road	Arterial street	93	186
Moderate traffic road	Collector street	83	156
Low traffic road	Feeder street	77	170
Other	Mixed	59	36

3. Results

3.1. Sediment accumulation patterns

Laboratory experiments showed consistent patterns of sediment accumulation, with most of the sediment introduced to the BMPs deposited at the bottom of the enclosures in both the *Long* and *Mini* BMPs (Fig. 1). Examination of the enclosures and BMP media at the conclusion of the experiments showed minimal sediment accumulation on the surface, void spaces, or along the sides of the BMP. The fine sediment gradually accumulated as stormwater was loaded to the BMPs, eventually forming a layer approximately 2–8 mm thick at the base of the enclosures (Fig. 2). Although the *Mini* configuration provided lateral infiltration opportunity, very little material was found accumulated on the side infiltration surfaces, even as thought the bottom clogged rapidly. We found no evidence that sediment accumulation locations varied based on the timing of stormwater applications or installation of filter fabric at the media interface.

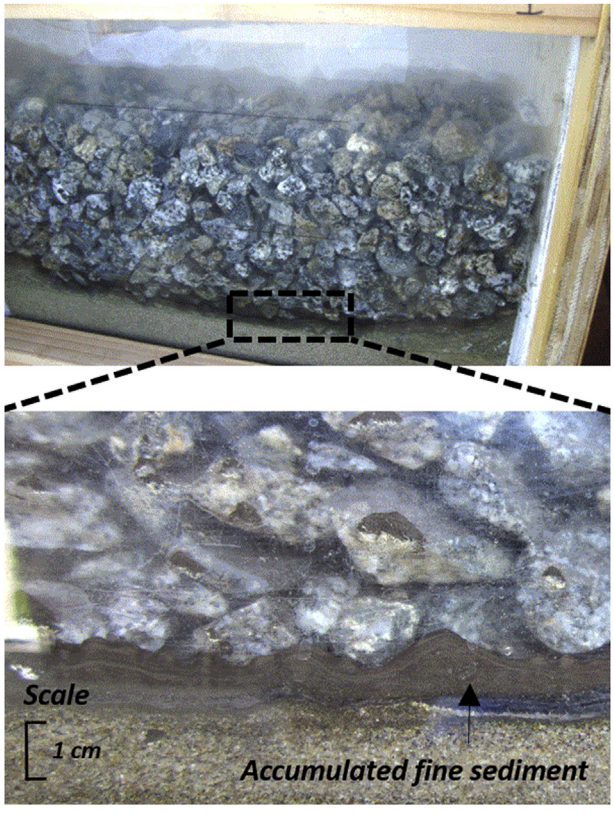

Fig. 2. Accumulation of fine sediment at the base of the BMP media. Image is near the end of an experiment with approximately 500 g of sediment loaded.

3.2. Infiltration rate declines

Laboratory and field experiment results showed similar patterns of infiltration rate decline over time as a function of sediment loading: rapid initial reductions became more gradual as cumulative sediment loading increased (Fig. 3). The controlled setting of the laboratory experiments produced greater precision than the field-based experiments, which showed higher standard deviations between trials (Fig. 3). Initial and final infiltration rate of the BMPs varied depending on infiltration surface area and initial K_{sat} (Table 2): experiments with greater infiltration surface area and higher starting K_{sat} values required a greater cumulative mass of sediment to create comparable declines in infiltration rate. Nearly all the experiments showed declines to less than 20% of initial rates, and several retained only 10% of their original performance by the experiment end (Table 2).

Overall infiltration rate declines were greater when there was less lateral infiltration surface available, even as the total sediment loading per infiltration surface increased (Table 2), indicating that BMP geometry may play an important role in the overall infiltration rate decline. The experimental results showed that the more lateral infiltration surface that was available in a BMP, the slower the decline in infiltration rate. The laboratory enclosures had either no side infiltration (*Long*) or two side infiltration surfaces available (*Mini*), while the field-based experiments had four sides available for infiltration. As a result of the different BMP geometries, infiltration rates decline as a function of sediment loading (g/m^2) were most severe in *Long*, followed by *Mini*, followed by the field-based BMPs. The *Mini* BMPs sustained better infiltration performance with more cumulative sediment loading compared to the *Long* BMPs even though these BMPs had less total infiltration surface area available (Table 2).

The *Long* BMPs showed little difference in total infiltration rate decline by experiment end whether or not filter fabric (FF) was installed, but their trajectories diverged significantly (Fig. 3). During the first half of the experiments, filter fabric installed in the *Long* BMPs resulted in less infiltration performance decline. Non-overlapping confidence intervals around the mean values in Fig. 3 indicate that the difference between these two decline trajectories is significantly different at the 90% level. After approximately 750 g/m^2 of fine sediment were loaded, the difference with and without filter fabric was no longer discernible. Comparisons of the field-based BMPs in Kings Beach also included trials with and without filter fabric, with similar results to the laboratory experiments: less initial infiltration rate decline for the filter fabric configuration and a similar total infiltration rate decline by experiment end (Fig. 3).

A comparison of the field experiments in Kings Beach and Seabright Beach sand allowed inspection of the influence of

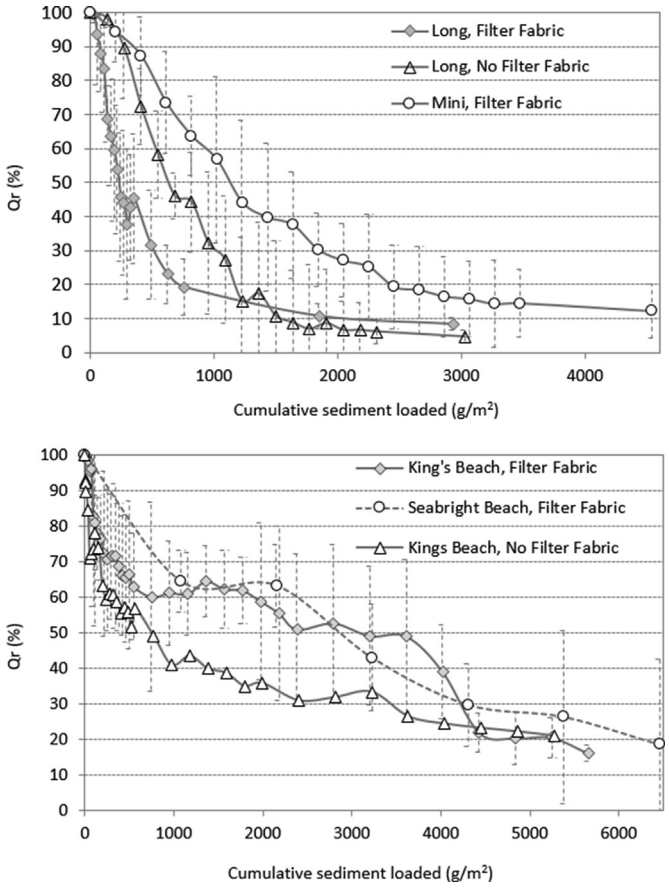

Fig. 3. BMP Infiltration capacity declines as a function of cumulative sediment loading for laboratory and field experiments with and without filter fabric installed. Points show average values for experimental triplicates and error bars show 95% confidence intervals.

surrounding soil permeability on infiltration rate declines. Both showed similar infiltration rate declines (Fig. 3) even though the K_{sat} of the Kings Beach soil (15 cm/h) was much lower than that of the Seabright Beach site (38 cm/h). So, while the absolute infiltration rate of a BMP installed in sand at Seabright Beach is much greater than the same BMP installed in the Kings Beach site, infiltration performance loss relative to initial performance did not vary significantly as a function of the initial K_{sat} of underlying material.

3.4. Vertical and lateral infiltration components

Exponential regression curves using the triplicate measurements for each experiment explain a similar amount of variance for each set of points: *Long* (R^2 = 0.86), *Mini* (R^2 = 0.82) (Fig. 4). Regression parameter estimates for the equations shown in Fig. 4 are provided in Table 3 along with their calculated standard errors for *Long* and *Mini*. Using Equation (4), we calculated the lateral component of the infiltration rate decline (Qr_l) for the *Mini* BMP at each measurement interval. The resulting calculated curve is plotted in Fig. 4 along with the measured *Long* and *Mini* infiltration rate (Qr), showing the shallower decline trajectory for the lateral infiltration component.

Using the resulting regression coefficients, we calculated infiltration rate declines for the vertical and lateral infiltration surfaces of the Kings Beach field sites. With the ratio of vertical to lateral infiltration surfaces for the field BMPs experiments (1:4), we predicted their overall infiltration rate declines. The resulting predictions are shown in Fig. 5 along with all field measurements for both Kings Beach and Seabright Beach field sites. The predicted curve for overall infiltration rate decline is somewhat steeper than the best fit curve for the aggregate data set (R2 = 0.54). The predicted values lie outside of the 95% confidence interval of the regression curve fit (Fig. 5), but well within the prediction interval of this curve which reflects the wide data scatter. This rough correspondence with the observed data provides initial support for the application of this method to other BMP sizes and locations.

3.5. Predicting BMP performance declines

Outputs from TELR show a range of sediment loading, infiltration rate loss, and attenuation of stormwater infiltration benefits that depend on the location of each BMP. Sediment loading patterns throughout the drainage area are primarily determined by land use, impervious cover, and soil types, with annual of sediment loading (<125 μm) of approximately 40–17,000 g per year (Fig. 6). As we expect, higher sediment loading rates resulted in more rapid BMP infiltration rate declines, driven by the empirical exponential decline curves derived from the laboratory experiments. Compared to the Shallow BMP scenario, the Deep BMP scenario showed less overall infiltration performance decline as a result of the slower clogging rates associated with lateral infiltration surfaces. (Fig. 6). Mean infiltration performance remaining for 50 BMPs after 10 years of loading was only 6.9% for the Shallow scenario and 30.4% for the Deep scenario, which also showed greater variance across BMPs (Table 4). BMP infiltration performance remaining for the Shallow BMP scenario had a range of 0.1%–26.3% and the Deep BMP Scenario ranged from 6.6% to 60.1% (Table 4).

The Shallow and Deep BMP scenarios show distinct spatial patterns of runoff reductions after 10 years of sediment loading due to variations in land use and runoff generation, both of which cause overall performance declines (see Fig. 7). Runoff reductions for the entire catchment, with all BMPs initially capturing the runoff volume generated by the 85th percentile storm (3441 m^3), declined to 981 m^3 (69% decline) in the Deep BMP scenario and to 212 m^3 (93% decline) for the Shallow BMP scenario (Fig. 7). While 46 of the 50 BMPs in the Shallow BMP scenario showed runoff reductions <20% of their initial levels, the Deep BMP scenario only had 16 BMPs with a final performance below that level. All BMPs in the Shallow BMP scenario showed greater performance reductions compared to the Deep BMP scenario, but BMPs with higher loading showed smaller differences between the two geometries. This is because the highest loading Deep BMPs have attenuated to less than 7% of their original performance after 10 years (Table 4), and since both governing curves for Shallow and Deep BMPs approach an asymptote, with very high loading the difference between them can become very small. The impact on the modeling outputs is greater sensitivity to BMP geometry differences where sediment loading is lower (relative to BMP infiltration surface area).

4. Discussion

4.1. Measuring BMP performance declines

The rapid rate of estimated infiltration BMP performance declines indicated by the results are somewhat disconcerting, but largely consistent with previous work. The pattern and magnitude of infiltration rate declines observed in the laboratory experiments appear to be comparable with observations by Siriwardene et al. (2007a), who used a similar experimental setup and found an 80% infiltration performance reduction after 375 g/m^2 of sediment loading. While Siriwardene et al. (2007a) loaded an order of

Table 2
Final infiltration rates and experimental parameters for laboratory and field experiments with and without filter fabric (FF).

		Laboratory			Field		
		Long, (No FF)	Long (FF)	Mini (FF)	Kings Beach (FF)	Kings Beach (FF)	Seabright Beach (FF)
Qr (%)	Trial 1	6.1	9.2	7.2	32.4	15.1	13.4
	Trial 2	5.7	7.1	12.9	12.2	16.9	18.2
	Trial 3	2.0	8.8	16.6	18.5	17.4	–
	Trials Mean	4.6	8.4	12.2	21.0	16.5	15.8
	Configuration Mean	6.5		12.2	18.0		
A_{inf} (m^2)		0.07		0.05	0.37		
Sediment loading (g/m^2)		3000		4500	6400		
A_{side}: A_{base}		0		1:1*	4:1		

*Half of each of the 2 *Mini* BMP sides are blocked by Plexiglass and not available for infiltration (see Fig. 1).

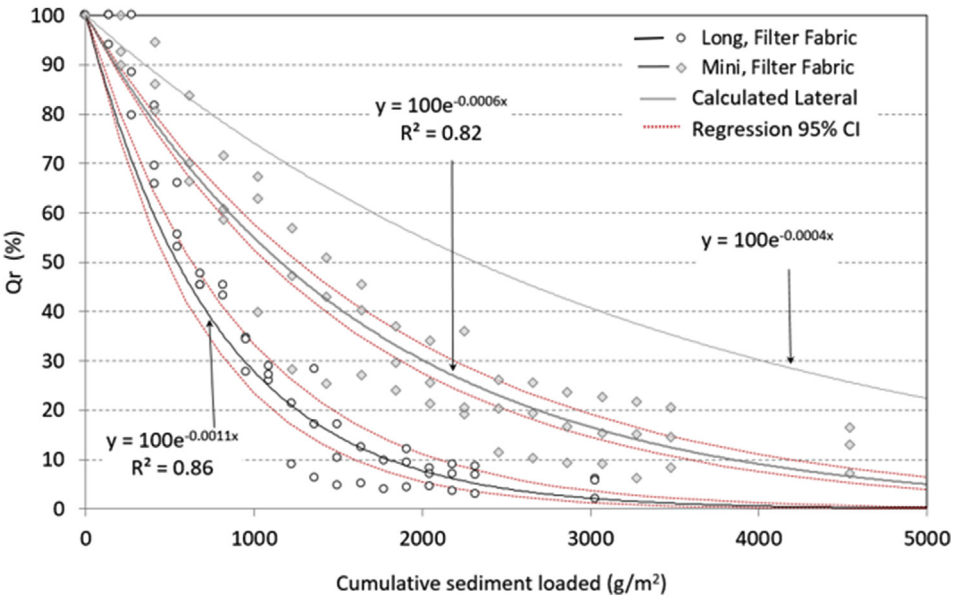

Fig. 4. Infiltration rate decline curves for the Long and Mini BMPs with the lateral decline calculated as the difference between the two curves, Exponential regression curves fit to each data set rely on the same data shown in Fig. 3.

Table 3
Regression parameters and standard errors for measured performance decline curves.

	Parameter Estimate	Std. Error	95% CI
Long	0.0011	0.000046	(0.00106, 0.00123)
Mini	0.0006	0.000021	(0.00056, 0.00064)
Lateral	0.0004	–	–

magnitude less sediment mass to their infiltration BMPs, their stormwater only included material <6 μm, which was estimated to make up only 1–10% of the total sediment loads (Siriwardene et al. 2007a,b,c). Field studies also provide evidence of rapid initial performance declines, including Emerson et al. (2010) who found that infiltration performance declined 90% in the first year of installation of infiltration BMPs, Brown and Borst (2014) found a decrease of 80% from the initial infiltration rate within the first year in one part of their infiltration trench, and Warnaars et al. (1999) found declines between 30 and 70% within 2–3 years. In contrast, Toran and Jerzejczyk (2017) did not show similar performance declines in their infiltration trenches over 2.5 years, but comparisons are difficult since the mass of sediment or fine particle loading was not measured in these experiments.

Representation of real-world BMP conditions of in controlled experiments is challenging due to potential effects of stormwater delivery timing and local soil dynamics. While soil composition may affect infiltration rate declines, the fact that the field experiments showed declines to be insensitive to the initial infiltration rates (see Fig. 3, bottom graph) provides evidence that the observed patterns may be applicable to other soil types. We caution though, that because the field experiments were conducted only over a period of weeks, they may not realistically represent the wetting and drying of the soil on BMP media over longer time periods which may also affect clogging rates (Kandra et al., 2010). Likewise, temperature fluctuations can affect soil moisture dynamics, and variable flow conditions will control the composition and timing of sediment delivery. Use of larger size material (e.g. >125 μm) in our experiments may have provided a more realistic stormwater composition since it can create clogging at the surface and within the void spaces of the media as observed by Mercado et al. (2015) and Sobotkova et al. (2018). However, use of only fine material likely allowed for a more precise measurement of clogging impacts since fine sediment particles are the most important factors in the clogging process in these types of BMPs (Siriwardene et al., 2007b).

Applicability of the results will be limited to BMPs similar to those used in the experiments and subject to the uncertainty

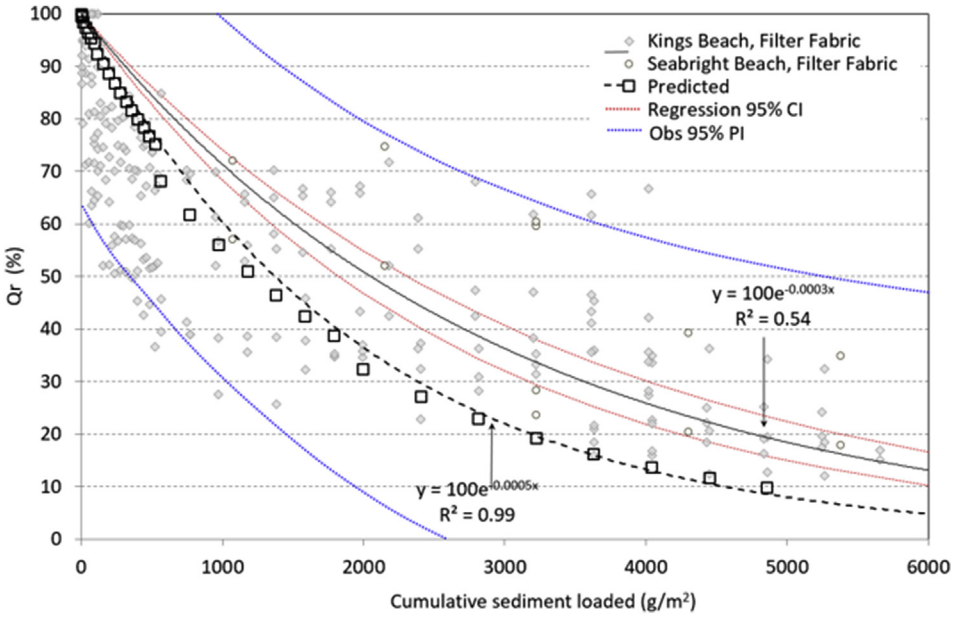

Fig. 5. Infiltration capacity declines for BMPs at the two field sites (all data shown) with exponential regression curves fitted. Boxes show the predicted infiltration capacity decline based on the measured vertical and calculated lateral infiltration components. Confidence intervals (CI) for the measured data are shown along with prediction intervals (PI) for new values.

associated with transporting empirical curves in the laboratory to the field. Different clogging mechanisms may dominate in BMPs that do not use gravel, since smaller clasts can more easily trap sediment particles higher up in a BMP, rather than only at the infiltration surface. Divergence of the two curves in Fig. 5 likely reflects both measurement error as well as dissimilarity of laboratory and field experimental conditions, such as differences in wetting front development below the BMP media. Given that predicted performance declines were somewhat steeper than the best fit curve for the field data (Fig. 5), these outputs probably reflect conservative estimates of ongoing infiltration performance, and are best framed as a proof-of-concept at this stage.

4.2. BMP design and maintenance implications

The accumulation of fine sediment almost exclusively at the bottom of infiltration BMPs in the laboratory experiments has some important implications for BMP design and maintenance schedules. While performance attenuation of BMPs may be affected by several factors such as filter media and stormwater inflow characteristics (Kardra et al., 2010; Mays and Hunt, 2005; Skolasinska, 2006), our results highlight the influence of the infiltration BMP geometry on performance declines. With BMP sizing and sediment loading held constant, the rate of clogging was strongly influenced by the proportioning of vertical and lateral infiltration surfaces. While Siriwardene et al. (2007a) observed substantial sediment accumulation on the sides of an infiltration trench, field studies have indicated that infiltration at the base surface of an infiltration BMP may become negligible over a short period, while the sides remain active (Emerson et al., 2010; Toran and Jedrzejczk, 2017).

Our findings support the concept that stormwater infiltration BMP designs with more lateral infiltration surface may extend the lifespan of infiltration systems and allow longer intervals between required maintenance. The accumulated layer at the infiltration surfaces effectively reduces the hydraulic conductivity of the boundary through which water must move to exit the BMP (e.g. Hatt et al., 2008). Retention of higher infiltration rates on the sides of BMPs due to less material accumulation may be good news for designers of green stormwater infrastructure to meet urban low impact development standards, since deeper BMPs can occupy smaller footprints in tight spaces. However, the performance benefit of making infiltration trenches narrower and deeper will reach a limit dictated by the hydraulics of a BMP footprint needed to capture a required volume of stormwater.

4.3. Incorporation of results to catchment modeling systems

A key advantage of using a model like conceptual model like TELR, is greater capacity to efficiently incorporate granular spatial patterns of the factors that drive BMP performance declines over time. Physically-based descriptions of clogging (e.g. Browne et al., 2008) are difficult to adopt due to their level of detail and associated data requirements to support parameterization (Petrucci and Bonhomme, 2014). This makes implementation in a spatially distributed framework impractical due to computational costs along with expertise and data requirements, such as identifying and validating parameters for pollutant build-up and wash-off processes (Freni et al., 2009). Like the current study, Siriwardene et al., (2007a,b,c) incorporated their laboratory results to the conceptual MUSIC catchment modeling system (Wong et al., 2005) to predict clogging rates and estimate the lifespan of infiltration systems. Like TELR, MUSIC employs a stochastic rainfall representation to simplify calculations and make the model easier to use (Wong et al., 2002), but unlike TELR, MUSIC lacks the ability to explicitly represent spatial variation of catchment of factors that drive BMP clogging.

The results presented illustrate the utility of using empirical estimates of BMP performance in a spatially distributed catchment model supported by widely available data. Stormwater management is often done at the scale of parcels or neighborhoods, with managers prioritizing actions and allocating resources at this level. The model outputs shown in Figs. 6 and 7 align with this scale of decision making. They provide a stormwater manager with information about the relative risk of BMP clogging due to sediment

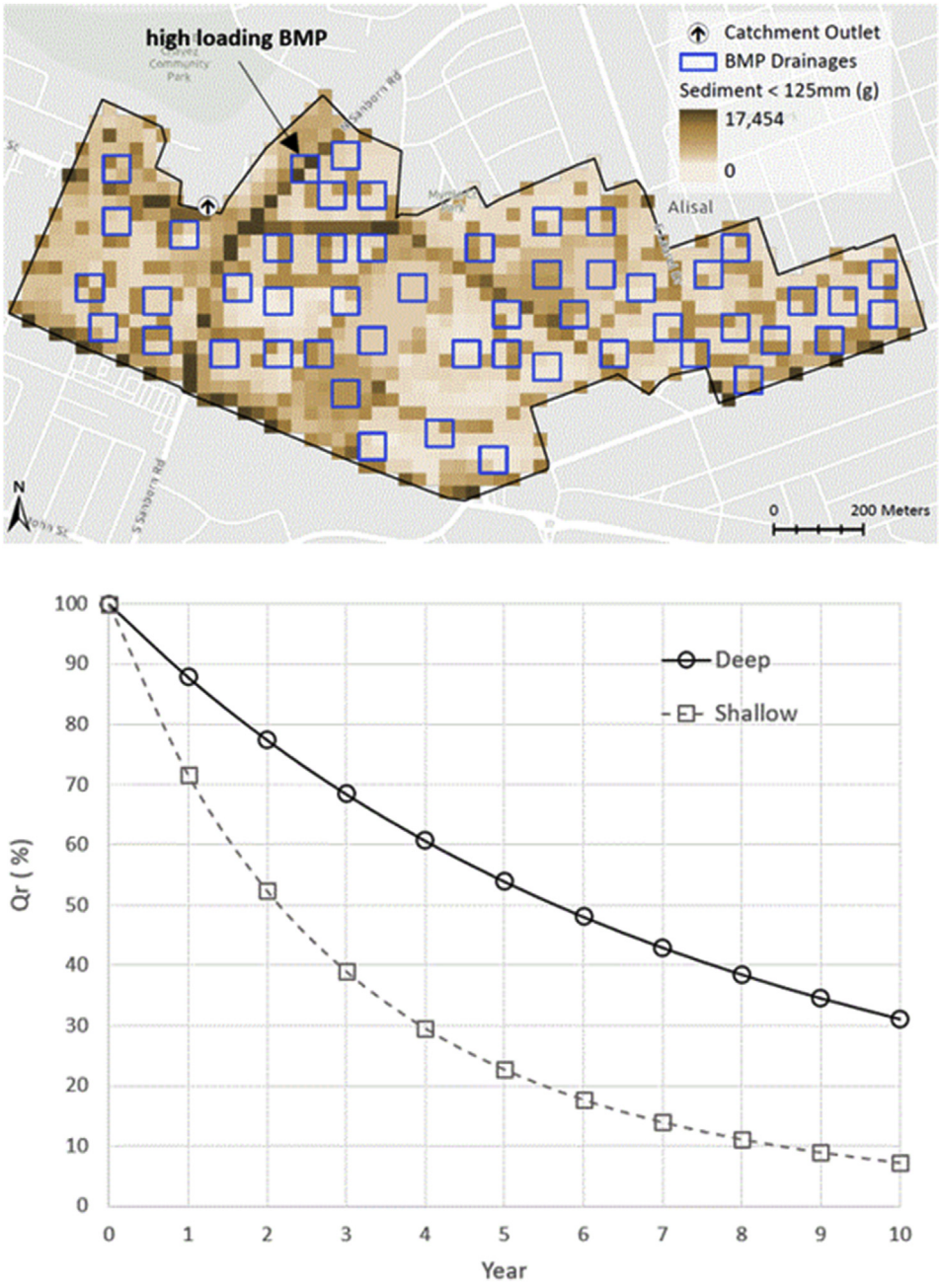

Fig. 6. Annual sediment loading outputs from the TELR model and BMP infiltration rates as a percent of their initial rate (Qr). Annual sediment loading rates (g) are shown with BMP drainage areas throughout a catchment in Salinas, CA. The plot shows mean outflow reductions (solid and dashed lines) for all 50 BMPs over a 10-year period.

Table 4
Statistical summary of initial and final runoff reductions after 10 years of sediment loading as a % of initial reductions for 50 BMPs.

	Mean	Std Dev	Max	Median	Min	n < 20%
Initial Annual Runoff Reduction (m^3)	68.8	2.8	131.4	69.2	23.1	–
Final Deep Runoff Reduction (%)	30.4	7.9	60.1	29.5	6.6	16
Final Shallow Runoff Reduction (%)	6.9	2.8	26.3	4.1	0.1	46

loading and how that may impact their expected runoff reductions and corresponding pollutant load reductions over time. BMPs that receive runoff from high loading areas can be flagged for maintenance checks more frequently than low loading areas (see example in Fig. 6). They also illustrate where implementing deeper BMPs with greater side infiltration area may provide the greatest benefits in terms of extending BMP maintenance schedules. Adjusting pollutant load reductions according to estimated BMP performance attenuation will provide a better alternative than assuming BMPs continue to function at a static design level in perpetuity

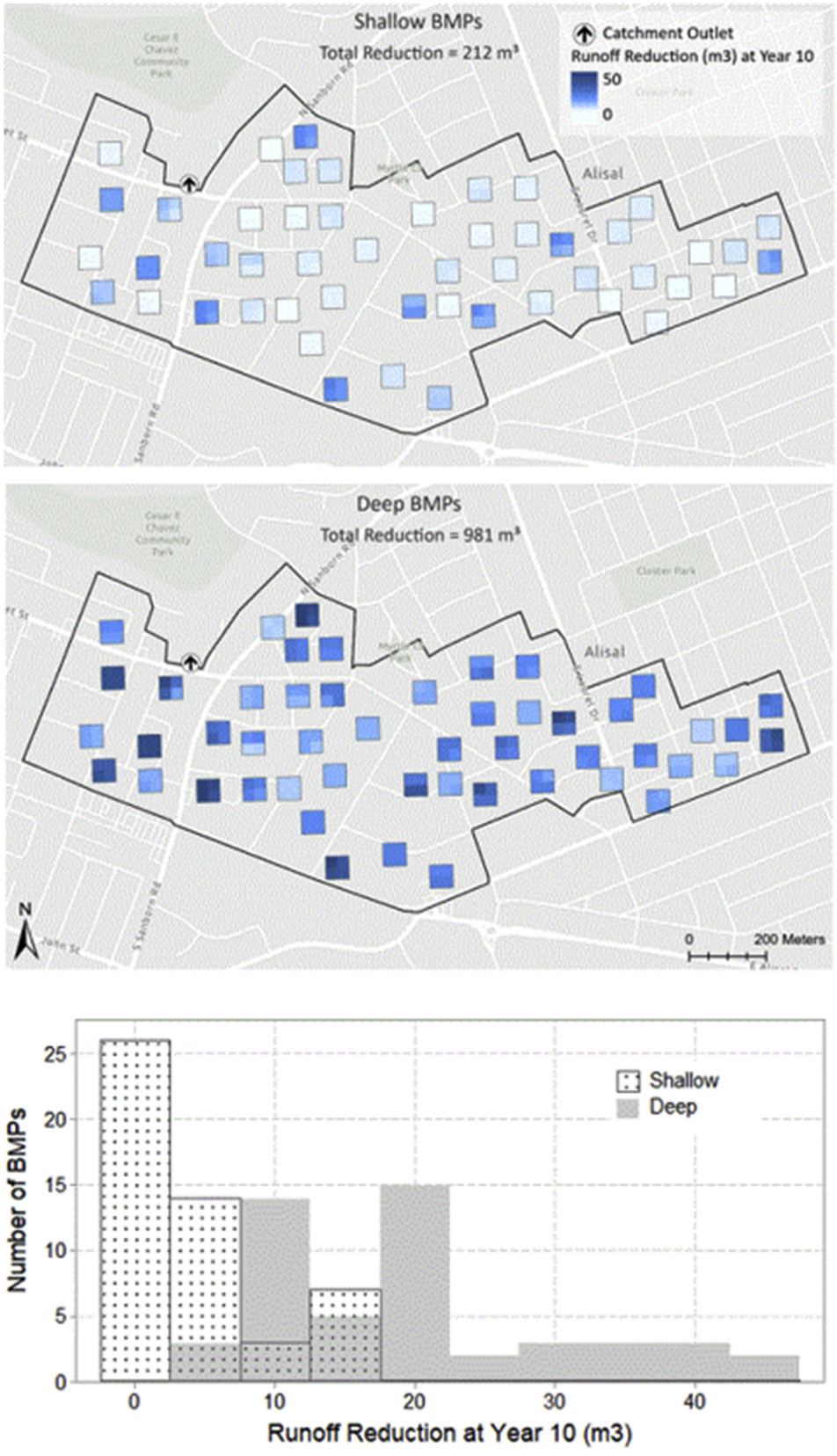

Fig. 7. Runoff reductions for Deep and Shallow BMP scenarios for a catchment in Salinas, CA with BMPs sized to capture the 85th percentile storm event. Maps show values calculated for 30 m grid cells and histograms show reductions for each BMP drainage area.

irrespective of maintenance attention. In combination with monitoring data, such information can help align our intuitions about the scale of urban water quality problems relative to the resources currently available to cities to work towards water quality improvement goals.

As stormwater programs move towards integration of asset management and catchment stormwater modeling, there is the potential to bring better tools to decision makers to reliably communicate the environmental value of their stormwater treatment infrastructure. Of course, the sources of uncertainty already discussed propagate into the model outputs, which must be considered, if they are to be used as the basis for decision making. As the relationships identified in this work are further refined with additional measurements, they will be incorporated web-based stormwater planning software previously reported in Beck et al. (2017) and Conley et al. (2019) (www.2nform.com). The revised algorithms will allow the relevant parameters to be handled dynamically with local sediment delivery to BMPs modeled based on site specific characteristics, and BMP sizing and drainage defined as inputs via a user interface.

5. Conclusions

Stormwater BMP infiltration rates showed similar patterns of rapid initial decline as a function of sediment loaded per infiltration surface area (g/m^2), regardless of soil setting or stormwater sediment concentration. Filter fabric appeared to preserve some infiltration performance during initial loading, but final declines were similar with or without it. The experimental results showed that BMP geometry strongly influenced the BMP infiltration decline trajectories and is a more important determinant on the total infiltration rate loss than either filter fabric installation or initial soil infiltration rate. As evidenced by visual inspections of the BMP enclosures, this appears to be due to the accumulation of most sediments the base of BMPs rather than within the BMP media or along the sides, even when more lateral infiltration surface is available than base infiltration surface. Clogging of the BMP bottom infiltration surface appears to a primary factor controlling the observed BMP infiltration rate declines. Ongoing experimental work will focus on field verification of BMP clogging rates, and relationships between sediment loading rates and BMP geometry.

Stormwater managers and water quality regulators need better information to make wise decisions about how to optimize BMP implementation and allocate maintenance resources to achieve the greatest overall water quality benefits. As greater accountability is demanded of stormwater managers in the future, practical methods to ensure that pollution load reduction estimates reported to regulators are reasonable and allow them to allocate maintenance resources efficiently are of growing importance. Given the rapid performance declines associated with high sediment loading rates, cost trade-offs between infiltration systems and source control measures such as effective and strategic street sweeping programs may be evaluated in high loading drainages. Incorporation of experimental results to web-based catchment modeling systems can allow non-modeling experts to evaluate such scenarios and extend the utility of this type of work support ongoing stormwater program improvement.

Funding

This work was supported through funding from the Tahoe Regional Planning Agency (http://www.trpa.org/), Stateline, NV USA.

Declaration of competing interest

The authors declare that they have no known competing financial interests or personal relationships that could have appeared to influence the work reported in this paper.

References

2NDNATURE, 2017. Stormwater Tool to Estimate Load Reductions, p. 145. Final Technical Document. July 2018.
2NDNATURE and Northwest Hydraulic Consultants, 2013. Infiltration BMP Design and Maintenance Study. prepared for Tahoe Regional Planning Agency. March 2013.
Afrooz, N., Beck, M., Hale, T., McKee, L., Schiff, K., 2019. BMP performance monitoring to support reasonable assurance analysis, p. 45. Technical Report # 1081, July, 2019.
Ahiablame, L.M., Engel, B.A., Chaubey, I., 2012. Effectiveness of low impact development practices: literature review and suggestions for future research. Water Air Soil Pollut. 223 (7), 4253–4273.
Arnold Jr., C.L., Gibbons, C.J., 1996. Impervious surface coverage: the emergence of a key environmental indicator. J. Am. Plann. Assoc. 62 (2), 243–258. https://doi.org/10.1080/01944369608975688.
Beck, N.G., Conley, G., Kanner, L., Mathias, M., 2017. An urban runoff model designed to inform stormwater management decisions. J. Environ. Manag. 193, 257–269.
Bedan, E.S., Clausen, J.C., 2009. Stormwater runoff quality and quantity from traditional and low impact development watersheds. J. Am. Water Resour. Assoc. 45 (4), 998–1008. https://doi.org/10.1111/j.1752-1688.2009.00342.
Booth, D.B., Jackson, C.R., 1997. Urbanization of aquatic systems: degradation thresholds, stormwater detection, and the limits of mitigation. J. Am. Water Resour. Assoc. 33 (5), 1077–1090.
Brander, K.E., Owen, K.E., Potter, K.W., 2004. Modeled impacts of development type on runoff volume and infiltration performance. J. Am. Water Resour. Assoc. 40 (4), 961–970. https://doi.org/10.1111/j.1752-1688.2003.tb01572.x.
Brown, R.A., Borst, M., 2014. Evaluation of surface and subsurface processes in permeable pavement infiltration trenches. J. Hydrol. Eng. 20 (2), 04014041-12.
Browne, D., Deletic, A., Mudd, G., Fletcher, T.D., 2007. A new model for stormwater infiltration systems. NOVATECH 2007.
Browne, D., Deletic, A., Mudd, G.M., Fletcher, T.D., 2008. A new saturated/unsaturated model for stormwater infiltration systems. Hydrol. Process. 22, 4838–4849.
Burton, G.A., Pitt, R.E., 2002. Stormwater Effects Handbook - A Toolbox for Watershed Managers, Scientists, and Engineers. Lewis publishers.
Clary, J., Strecker, E., Leisenring, M., Jones, J., 2017. International stormwater BMP database: new tools for a long-term resource. Proc. Water Environ. Fed. 2017 (15), 737–746.
Conley, G., Beck, N., Riihimaki, C.A., Hoke, C., 2019. Improving urban trash reduction tracking with spatially distributed Bayesian uncertainty estimates. Comput. Environ. Urban Syst. 77, 101344.
Dechesne, M., Barraud, S., Bardin, J.P., 2005. Experimental assessment of stormwater infiltration basin evolution. J. Environ. Eng. 131 (7), 1090.
Ellis, J.B., 2000. Infiltration systems: a sustainable source-control option for urban stormwater quality management? J. Char. Inst. Water Environ. Manag. 14 (1), 27–34.
Emerson, C.H., Wadzuk, B.M., Traver, R.G., 2010. Hydraulic evolution and total suspended solids capture of an infiltration trench. Hydrol. Process.: Int. J. 24 (8), 1008–1014.
EPA, 2009. Technical Guidance on Implementing the Stormwater Runoff Requirements for Federal Projects under Section 438 of the Energy Independence and Security Act, p. 63.
Field, R., Tafuri, A.N. (Eds.), 2006. The Use of Best Management Practices (BMPs) in Urban Watersheds. DEStech Publications, Inc.
Fletcher, T.D., Duncan, H.P., Poelsma, P., Lloyd, S., 2003. Stormwater Flow and Quality and the Effectiveness of Non-proprietary Stormwater Treatment Measures: A Review and Gap Analysis. The Institute for Sustainable Water Resources, Monash University and the CRC for Catchment Hydrology, Victoria.
Freni, G., Mannina, G., Viviani, G., 2009. Stormwater infiltration trenches: a conceptual modeling approach. Water Sci. Technol. 60 (1), 185–199.
Freni, G., Mannina, G., Viviani, G., 2010. Evaluation of the effect of soil type on the infiltration trench clogging: a long term approach. NOVATECH 2010.
Furumai, H., Jinadasa, H.K.P.K., Murakami, M., Nakajima, F., Aryal, R.K., 2005. Model description of storage and infiltration functions of infiltration facilities for urban runoff analysis by a distributed model. Water Sci. Technol. 52 (5), 53–60.
Gilroy, K.L., McCuen, R.H., 2009. Spatio-temporal effects of low impact development practices. J. Hydrol. 367 (3), 228–236. https://doi.org/10.1016/j.jhydrol.2009.01.008.
Grove, N.E., Edwards, R.T., Conquest, L.L., 2001. Effects of scale on land use and water quality relationships: a longitudinal basin-wide perspective. J. Am. Water Resour. Assoc. 37 (6), 1721–1734. https://doi.org/10.1111/j.1752-1688.2001.tb03672.x.
Hatt, B.E., Fletcher, T.D., Deletic, A., 2007. Treatment performance of gravel filter media: implications for design and application of stormwater infiltration systems. Water Res. 41 (12), 2513–2524.

Hatt, B.E., Fletcher, T.D., Deletic, A., 2008. Hydraulic and pollutant removal performance of fine media stormwater filtration systems. Environ. Sci. Technol. 42 (7), 2535–2541.
Holman-Dodds, J.K., Bradley, A.A., Potter, K.W., 2003. Evaluation of hydrologic benefits of infiltration based urban stormwater management. J. Am. Water Resour. Assoc. 39 (1), 205–2015. https://doi.org/10.1111/j.1752-1688.2003.tb01572.x.
Kandra, H., McCarthy, D., Deletic, A., Fletcher, T.D., 2010. Assessment of clogging phenomena in granular filter media used for stormwater treatment. NOVATECH 2010.
Kandra, H.S., McCarthy, D., Fletcher, T.D., Deletic, A., 2014. Assessment of clogging phenomena in granular filter media used for stormwater treatment. J. Hydrol. 512, 518–527.
Le Coustumer, S., Barraud, S., 2006. Long-term hydraulic and pollution retention performance of infiltration systems. In: 4th International Conference in Urban Drainage Modelling and 7th International Conference in Water Sensitive Urban Drainage, Melbourne, vol. 1, pp. 203–210.
Le Coustumer, S., Fletcher, T.D., Deletic, A., Barraud, S., 2007. Hydraulic Performance of Biofilters: First Lessons from Both Laboratory and Field Studies. NOVATECH, Lyon, France, 24th-28th June 2007.
Lindsey, G., Roberts, L., Page, W., 1992. Inspection and maintenance of infiltration facilities. J. Soil Water Conserv. 47 (6), 481–486.
Mays, C.M., Hunt, J.R., 2005. Hydrodynamic aspects of particle clogging in porous media. Environ. Sci. Technol. 39, 577–584.
Mercado, J.M.R., Maniquiz-Redillas, M.C., Kim, L.H., 2015. Laboratory study on the clogging potential of a hybrid best management practice. Desalination Water Treat. 53 (11), 3126–3133.
National Research Council (NRC), 2008. Urban Stormwater Management in the United States: Committee on Reducing Stormwater Discharge Contributions to Water Pollution. National Academies Press, Washington, DC, p. 598.
Nozi, T., Mase, T., Murata, K., 1999. Maintenance and management aspect of stormwater infiltration system. In: Paper Presented at the Proceedings of the Eighth International Conference on Urban Storm Drainage, Sydney, Australia, pp. 1497–1503.
Petrucci, G., Bonhomme, C., 2014. The dilemma of spatial representation for urban hydrology semi-distributed modelling: trade-offs among complexity, calibration, and geographical data. J. Hydrol. 517, 997–1007.
Pitt, R., Maestre, A., Morquecho, R., 2004. The National Stormwater Quality Database (NSQD), Version 1.1. University of Alabama, Tuscaloosa, AL.
Pitt, R.E., Clark, S.E., Eppakayala, V.K., Sileshi, R., 2016. Don't throw the baby out with the bathwater: sample collection and processing issues associated with particulate solids in stormwater. J. Water Manag. Model. 25, C416. https://doi.org/10.14796/JWMM.C416.
Pokrajac, D., Deletic, A., 2002. November. Clogging of infiltration drainage systems. In: International Conference on Sewer, Operation and Maintenance, Bradford, UK.
Potter, K.W., 2006. Small-scale, spatially distributed water management practices: implications for research in the hydrologic sciences. Water Resour. Res. 42, 2.
Rossman, L., Huber, W., 2015. Storm Water Management Model Reference Manual Volume I, Hydrology. US EPA Office of Research and Development, Washington, DC. EPA/600/R-15/162A, 2015.
Segismundo, E., Kim, L.H., Jeong, S.M., Lee, B.S., 2017. A laboratory study on the filtration and clogging of the sand-bottom ash mixture for stormwater infiltration filter media. Water 9 (1), 32.
Selbig, W.R., 2015. Characterizing the distribution of particles in urban stormwater: advancements through improved sampling technology. Urban Water J. 12 (2), 111–119.
Selvakumar, A., Muthukrishnan, S., Madge, B., Field, R., Tafuri, A., 2005. The Use of Best Management Practices (BMPs) in Urban Watersheds.
Shoemaker, L., Riverson, J., Alvi, K., Zhen, J.X., Paul, S., Rafi, T., 2009. SUSTAIN: a Framework for Placement of Best Management Practices in Urban Watersheds to Protect Water Quality. National Risk Management Research Laboratory, Office of Research and Development, US Environmental Protection Agency, Washington, DC.
Siriwardene, N.R., Deletic, A., Fletcher, T.D., 2007a. Preliminary studies of the development of a clogging prediction method for stormwater infiltration systems. Water Pract. Technol. 2 (2). Jun 1.
Siriwardene, N.R., Deletic, A., Fletcher, T.D., 2007b. Clogging of stormwater gravel infiltration systems and filters: insights from a laboratory study. Water Res. 41, 1433–1440.
Siriwardene, N.R., Deletic, A., Fletcher, T.D., 2007c. Modelling of Treatment of Solids through Infiltration Systems. NOVATECH 2007, Lyon, France.
Skolasinska, K., 2006. Clogging microstructures in the vadose zone- laboratory and field studies. Hydrogeol. J. 14, 1005–1017.
Sobotkova, M., Dusek, J., Alavi, G., Sharma, L., Ray, C., 2018. Assessing the feasibility of soil infiltration trenches for highway runoff control on the Island of Oahu, Hawaii. Water 10 (12), 1832.
Tang, A., Engel, B.A., Pijanowski, B.C., Lim, K.J., 2005. Forecasting land use change and its environmental impact at watershed scale. J. Environ. Manag. 76 (1), 35–45. https://doi.org/10.1016/j.jenvman.2005.01.006.
Toran, L., Jedrzejczyk, C., 2017. Water level monitoring to assess the effectiveness of stormwater infiltration trenches. Environ. Eng. Geosci. 23 (2), 11.
Tu, M.C., Traver, R., 2018. Clogging impacts on distribution pipe delivery of street runoff to an infiltration bed. Water 10 (8), 1045.
U.S. Department of Agriculture (USDA), Natural Resources Conservation Service (NRCS), 2007. Soil survey of the Tahoe basin area, California and Nevada. http://soils.usda.gov/survey/printed_surveys.
US EPA, 1983. Final Report. Results of the Nationwide Urban Runoff Project. Washington, DC.
US EPA, 2013. Our Built and Natural Environments: A Technical Review of the interactions between Land Use, Transportation, and Environmental Quality, second ed. EPA 231-K-13-001.
US EPA, 2017. Developing Reasonable Assurance: A Guide to Performing Model-Based Analysis to Support Municipal Stormwater Program Planning, p. 51.
US EPA, 2018. Improving Stormwater Program Monitoring, Evaluation, Tracking, and Reporting. Workshop Report and Recommendations, vol. 9. US EPA Region, San Francisco, CA, p. 65pp.
US EPA, 2019. BASINS 4.5 (Better Assessment Science Integrating Point & Non-point Sources) Modeling Framework. National Exposure Research Laboratory, RTP, North Carolina. (Accessed 8 September 2019).
USDA-SCS (U.S. Department of Agriculture-Soil Conservation Service), 1986. Urban Hydrology for Small Watersheds, second ed. USDA SCS, Springfield, Virginia. Technical release 55, NTIS PB87-101580.
Warnaars, E., Larsen, A.V., Jacobsen, P., Mikkelsen, P.S., 1999. Hydrologic behaviour of stormwater infiltration trenches in a central urban area during 2¾ years of operation. Water Sci. Technol. 39 (2), 217.
Wong, T.H., Fletcher, T.D., Duncan, H.P., Coleman, J.R., Jenkins, G.A., 2002. A model for urban stormwater improvement: conceptualization. In: Global Solutions for Urban Drainage, pp. 1–14.
Wong, T., Coleman, J., Duncan, H.P., Fletcher, T.D., Jenkins, G., Siriwardena, L., Taylor, A., Wootton, R., 2005. MUSIC Version 3.0. MUSIC Development Team, CRC for Catchment Hydrology, Melbourne.